Characterization and application of FRCM as a strengthening material for shear-critical RC beams

Adel Younis[1*], and *Usama* Ebead[2]

[1]PhD candidate, Department of Civil and Architectural Engineering, College of Engineering, Qatar University, Doha, Qatar
[2]Professor, Department of Civil and Architectural Engineering, College of Engineering, Qatar University, Doha, Qatar

Abstract. This paper investigates the effectiveness of fabric reinforced cementitious matrix (FRCM) systems in shear-strengthening of reinforced concrete beams. Three types of FRCM systems were considered, namely, polyparaphenylene benzobisoxazole (PBO)-FRCM, Carbon-FRCM, and Glass-FRCM. At first, tensile characterization test was performed on 15 FRCM coupons with the aim of identifying the tensile properties of the FRCM systems adopted. After that, seven shear-critical RC beams were tested under three-point loading, with the consideration of two test parameters: (a) FRCM material (glass/carbon/PBO); and (b) strengthening configuration (full/intermittent). The study results revealed the use of FRCM as a strengthening material to achieve a considerable improvement in the structural capacity of shear-critical RC beams. The average gain in the shear capacity of the FRCM-strengthened beams was 57%. The beam specimens strengthened with carbon-FRCM showed the highest improvement as compared to those strengthened with glass- and PBO-FRCM systems. As intuitively expected, the shear capacity improvement achieved with the full-length strengthening systems was generally higher than that with the intermittent counterparts.

1 Introduction

Structural damage is normally encountered in reinforced concrete (RC) structures subject to harsh environment or unexpected extra loads [1]. Consequently, different strengthening techniques of RC members were proposed to enhance their structural capacity such as ferrocement [2] and fibre reinforced polymer (FRP) [3–8]. Latterly, fabric reinforced cementitous matrix (FRCM) strengthening systems have emerged as a viable solution for structural rehabilitation and repair. FRCM consists of dry fibres embedded in an inorganic matrix, which is externally applied on the surface for the aim of strengthening RC and masonry structures [9,10].

FRCM systems have been successfully applied in the previous research for strengthening RC members such as slabs [11], columns [12–14], and beams critical in flexure [15,16] or in shear [17–20]. In these studies, a noticeable improvement was generally reported in the loading capacity of the FRCM-strengthened members as compared to that of the non-strengthened benchmarks. Nonetheless, it is well-agreed that a proper understanding of the tensile characteristics of the FRCM composite is required to complete the structural design or numerical modeling of the FRCM strengthening system [21–23].

In view of this, the current paper has a two-fold objective: (a) to investigate the effectiveness of FRCM systems in strengthening of shear-critical RC beams; (b) to enrich the literature with contextual data pertinent to the tensile characteristics of commercially available FRCM systems, which can be used for future applications in structural rehabilitation and repair. In this effort, the authors have considered three types of FRCM systems: Glass (G)-FRCM, Carbon (C)-FRCM, and polyparaphenylene benzobisoxazole (PBO)-FRCM. At first, tensile characterization test was performed on 15 FRCM test coupons to obtain the tensile properties of the utilized FRCM systems. After that, a total of seven RC beams critical in shear were tested under three-point loading to assess the efficacy of FRCM strengthening systems, while considering the FRCM type and strengthening configuration as test variables.

In the beginning, the experimental program will be explained in terms of materials description, test specimens, and test setup. After that, results and observations of this experimental study will be presented and discussed, mainly for the tensile characteristics of the FRCM systems as well as the structural performance of the strengthened RC beams.

2 Experimental methodology

2.1 Materials

Ready-mixed concrete with a 30-MPa average 28-day strength was used for casting the beam specimens. Beam specimens were reinforced with bars of grade 500B (BS 4449:2005 [24]). The average mechanical properties of the steel reinforcement based on tested samples are 595

---

* Corresponding author: adel.younis@qu.edu.qa

MPa for the yield stress, 0.266% for the yield strain, and 224 GPa for the modulus of elasticity.

Three types of FRCM systems were considered, which are: Glass-FRCM [25], Carbon-FRCM [26], and PBO-FRCM [27]. To prepare the FRCM composite, the textile was embedded in its corresponding mortar in accordance with the manufacturers' recommendations. The amount of mixing water needed per 25 kg of mortar was 5 litres for the Glass-FRCM and 7 litres for the Carbon- and PBO-FRCM systems. The mechanical properties for each textile type as provided by the manufacturers are listed in Table 1, including the textile area per unit width (A_f), ultimate strain (ε_u), elastic modulus (E), and tensile strength (σ_{fu}), along with the compressive strength of their associated mortars (f_c).

Table 1. Textile and mortar properties for the FRCM systems.

Textile type	A_f (mm²/mm)	E (GPa)	σ_{fu} (GPa)	ε_u (%)	f_c (MPa)
PBO	0.045	270	5.80	2.15	30
Carbon	0.047	240	4.80	1.80	20
Glass	0.047	80	2.60	3.25	40

2.2 Test specimens

2.2.1 FRCM tensile coupons

In accordance with AC434 [28], five tensile coupons were prepared for each FRCM system. A panel of 410 mm in length, 250 mm in width, and 10 mm in thickness was first cast on a flat wooden mould. After being cured for 28 days, each panel was cut to five number of 410-mm long, 50-mm wide, and 10-mm thick coupons. Each FRCM tensile coupon encompassed a single textile layer, of which the longitudinal direction was parallel to the coupon's length.
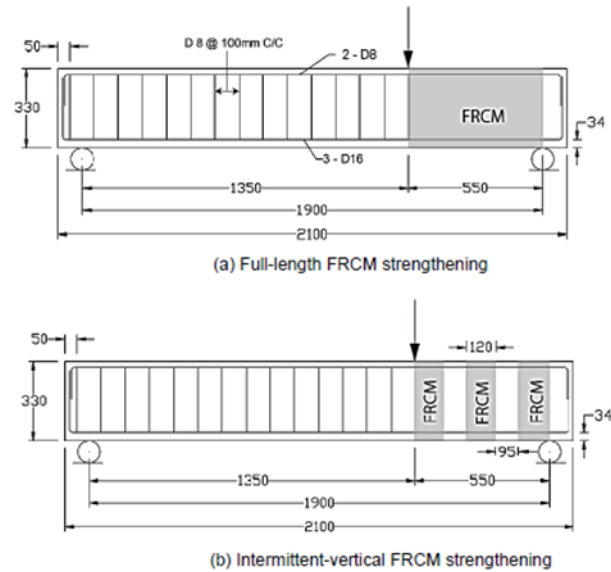
2.2.2 RC beam specimens

Seven 2100-mm long, 150-mm wide, and 330-mm deep reinforced concrete beams were tested. Bars of 16 mm in diameter were used as flexural reinforcement, while 8-mm diameter stirrups spaced at 100 mm were used as shear reinforcement in the non-critical regime. The beam specimens had no stirrups within the 550-mm long critical span as illustrated in Figure 1. One of the beam specimens was kept non-strengthened as a benchmark, while the rest were FRCM-strengthened within the critical shear span with different types and configurations (Figure 1). A 34-mm clear concrete cover was typically considered, leading to an effective depth of 280 mm in RC beam specimens.
Table 2 presents the test matrix of the RC beam specimens, in which two parameters were investigated:
(i) FRCM type: glass-, PBO-, and carbon-FRCM.
(ii) Strengthening configuration: the beam specimen was strengthened along the critical shear span either fully by a continuous FRCM plate or intermittently by a set of 120-mm wide FRCM strips spaced at 95 mm.

The FRCM system was applied on each side of the strengthened beam and composed of (i) an internal mortar layer of 5 mm in thickness, placed after roughening the concrete surface; (ii) two layers of textile separated by a 3-mm thick intermediate mortar layer; and (iii) an external layer of 5-mm thick mortar.

(a) Full-length FRCM strengthening

(b) Intermittent-vertical FRCM strengthening

Fig. 1. Elevations of the beam specimens with (a) full-length and (b) intermittent FRCM shear strengthening systems.

Table 2. Test matrix for the beam specimens.

| Beam ID	Textile material	Strengthening configuration
Reference	-	-
C-Full	Carbon	Full
C-Intermittent	Carbon	Intermittent
P-Full	PBO	Full
P-Intermittent	PBO	Intermittent
G-Full	Glass	Full
G-Intermittent	Glass	Intermittent

2.3 Test setup

2.3.1 Test setup for FRCM tensile characterization

The tensile characterization test setup for FRCM coupons is illustrated in Figure 2. Tensile load was uniaxially applied at a rate of 0.25 mm/min. Metal plates were attached to the specimen's ends using epoxy with a 150-mm bond length. The specimen was gripped by a double clevis-type connection from one end and a single clevis-type connection from the other. A clip-type displacement transducer was placed to continuously measure the extension of the test coupon. Hence, the FRCM strain can be calculated as the measured coupon's extension divided by the 200-mm extensometer length.

For each load step, the axial tensile stress can be determined as the recorded load (P) divided by the FRCM equivalent area. This FRCM equivalent area is actually

the average textile area per unit width (A_f), provided in Table 1 for each textile type, multiplied by the specimen's width (50 mm).
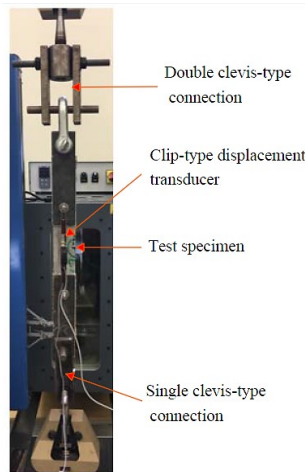
Fig. 2. Tensile characterization test setup.

2.3.2 Test setup for RC beams

**Fig. 3.** Test setup for RC beams.

RC beams were tested under three-point loading (Figure 3) using the Instron 1500HDX Static Hydraulic Universal Testing machine located in Qatar University Structures Laboratory. Loading was applied on the tested beams at a rate of 1 mm/min until failure. Strain gauges (with 5% maximum limit and 5-mm gauge length) were fixed to the longitudinal bars. The deflection was measured below the loading point at each step using a linear variable displacement transducer. Data acquisition of the measurements was done at a 1-Hz frequency range.

3 Results and discussions

3.1 Tensile characterization test results

Figure 4 shows a representative stress–strain diagram for each FRCM system. In general, the stress–strain diagram for a FRCM system is composed of two characteristic phases: (i) the prior-cracking stiff section phase represented by a steep curve; followed by (ii) a reduced-slope curve indicating the cracked section phase until failure. The initial stiffness of G-FRCM was observed to be lower than that of PBO-FRCM and C-FRCM. This can be attributed to the lower elastic modulus of glass textile as compared to that of PBO or carbon (Table 1).
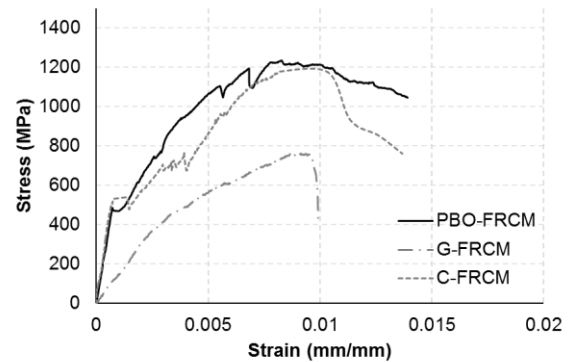
Fig. 4. Stress–strain diagrams for the FRCM systems adopted.

Table 3 lists the mean ultimate strain ($\varepsilon_{FRCM,u}$), tensile strength ($\sigma_{FRCM,u}$), cracked tensile modulus of elasticity (E_{FRCM}), and failure mode for the FRCM coupons. To calculate E_{FRCM} [28], a segment was considered between two data points at stress levels of $0.6\,\sigma_{FRCM,u}$ and $0.9\,\sigma_{FRCM,u}$ within the cracked-section curve. The slope of the line connecting these two points represents the cracked modulus of elasticity. The mean values of E_{FRCM} for G-FRCM, PBO-FRCM, and C-FRCM are 60 GPa, 112 GPa, and 135 GPa, respectively.

Table 3. Summary of the tensile characterization test results.

FRCM system	$\sigma_{FRCM,u}$ (MPa)	$\varepsilon_{FRCM,u}$ (%)	E_{FRCM} (GPa)	Failure mode*
G-FRCM	767	0.93	60	FR
PBO-FRCM	1235	1.06	112	FS
C-FRCM	1178	1.04	135	FS

*FS = Fabric Slippage; FR = Fabric Rupture

The G-FRCM system exhibited a more brittle failure behavior than that observed for the C-FRCM and PBO-FRCM counterparts. This can be evidenced by the harsh drop in the stress–strain diagram of G-FRCM at failure (Figure 4). Such observation can be explained by the relatively lower tensile strength of the glass textile compared to that of PBO or carbon (Table 1), which in turn results in the premature rupture of the textile inside the G-FRCM coupons. On the other hand, the Carbon-FRCM and PBO-FRCM systems generally showed a fabric-slippage type of failure. This explains the softening in the stress–strain curve after exceeding $\sigma_{FRCM,u}$.

All cracks were developed within the non-bonded area of the tensile coupons with no sign of slippage of the epoxy-bonded metal plates. The carbon-FRCM and PBO-FRCM systems have generally shown a higher number of cracks than that of the glass-FRCM counterpart. This can be probably attributed to the lower loading capacity of the glass-FRCM coupon than that of the carbon-FRCM and PBO-FRCM counterparts.

3.2 RC beam test results

Table 4 presents a summary of the test results for RC beam specimens. For each specimen, the second and the third columns of Table 4 list the ultimate load carrying capacity (P_u) and the gain in P_u as compared to that of the non-strengthened benchmark, respectively. As for the deformational characteristics, the deflection value (δ_u), the $\delta_u/\delta_{u,ref}$ ratio, and the flexural strain (ε_s) measured at failure are listed in the fourth, fifth, and sixth columns of Table 4, respectively.

Table 4. Summary of the RC beam test results.

Beam ID	P_u (kN)	Gain in P_u (%)	δ_u (mm)	$\dfrac{\delta_u}{\delta_{u,ref}}$	$\varepsilon_{s,u}$ (%)
Reference	104	-	3.25	-	0.143
C-Full	210	101.6	7.75	2.14	0.286
C-Intermittent	178	70.8	7.55	2.13	0.224
P-Full	151	45.5	5.35	1.65	0.195
P-Intermittent	138	32.4	4.6	1.42	0.170
G-Full	168	61.4	6.10	1.88	0.197
G-Intermittent	137	31.7	4.43	1.36	0.175

3.2.1 load carrying capacity

In general, the ultimate load carrying capacity for the FRCM-strengthened beams was higher than that of the benchmark specimen, demonstrating the successful application of the FRCM strengthening systems to enhance the structural capacity of shear-critical RC beams. The average improvement of the load carrying capacity after shear-strengthening was 86.2, 39.0, 46.6% for carbon, PBO, and glass FRCM systems, respectively. Figures 5-(a), (b), and (c) show the load–deflection diagrams for the beam specimens strengthened with carbon-, PBO-, and glass-FRCM systems, respectively.

The carbon-FRCM strengthening system generally showed better improvement in P_u than that of the PBO– and Glass-FRCM systems. The RC beams with full-length strengthening configuration exhibited significantly higher enhancement in P_u as compared to those with the intermittent strengthening configuration. This indicates the importance of the strengthening material's amount in the critical region. Furthermore, it was observed that using carbon-FRCM strengthening system was more effective in increasing the load carrying capacity of RC beams as compared to those with glass- and PBO-FRCM strengthening systems.

(a)

(b)

(c)
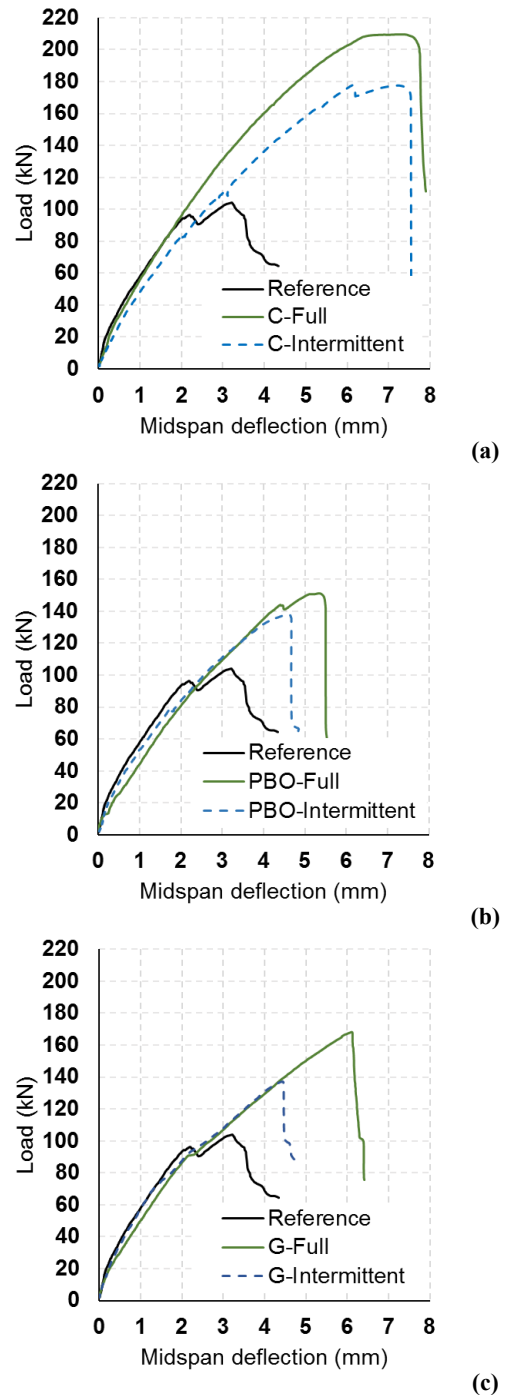
Fig. 5. Load–deflection plots for the beams with (a) Carbon-FRCM, (b) PBO-FRCM, and (c) Glass-FRCM strengthening systems.

3.2.2 Deformational characteristics

In general, the deflection measured at failure (δ_u) for the strengthened beams was higher than that of the benchmark specimen ($\delta_{u,ref} = 3.25\ mm$). The beams strengthened with carbon-FRCM systems exhibited higher values of δ_u than those measured for Glass- and PBO-FRCM counterparts, which can be an indication to a superior structural performance for the beams strengthened with carbon-FRCM systems. As an example, the C-Full specimen has a δ_u value of 7.75 mm, which is

higher than those measured for P-Full ($\delta_u = 5.35\ mm$) and G-Full ($\delta_u = 6.10\ mm$) specimens. In addition, the specimens with full-length strengthening configuration showed slightly higher values of δ_u compared to those with the intermittent strengthening. For instance, the P-Intermittent specimen has a δ_u value of 4.6 mm, which is lower than that measured for P-Full specimen ($\delta_u = 5.35\ mm$).

With reference to the flexural strain, all beam specimens have failed prior to the yield of the main steel ($\varepsilon_{s,u} < \varepsilon_y = 0.266\%$), with the exception of C-Full that has failed just after achieving the yield tensile strain ($\varepsilon_{s,u} = 0.286\%$). The $\varepsilon_{s,u}$ value for the FRCM-strengthened beams was commonly higher than that of the benchmark specimen, indicating the successful application of the FRCM system in postponing the brittle shear failure and, to some extent, allowing the main steel to be a little closer to the yield region.

4 Conclusions

This paper has investigated the effectiveness of FRCM systems in shear-strengthening of reinforced concrete beams. Three FRCM systems were considered, namely, carbon-FRCM, glass-FRCM, and PBO-FRCM. In the first part of this paper, tensile characterization test was performed on 15 FRCM coupons to measure the uniaxial tensile properties of the adopted FRCM systems. In the second part of this effort, a total of 7 RC beams were tested under three-point loading. Two test variables were considered, namely, the FRCM material and the strengthening configuration. Based on the study results, the following conclusions have been drawn:

- A typical shape was observed for the stress–strain diagrams of the FRCM tensile coupons with two distinct phases, of which the first is a steep curve indicating the non-cracked section, and the second is a gentle curve representing the cracked section.
- The cracked modulus of elasticity was calculated as 60 GPa, 112 GPa, and 135 GPa for glass-FRCM, PBO-FRCM, and carbon-FRCM, respectively.
- FRCM has been successfully used to improve the load carrying capacity of shear-critical RC beams. The average gain in the load carrying capacity achieved with FRCM-strengthening was 57%.
- A better strength improvement was reported for the full-length strengthening configuration than that of the intermittent counterpart.
- Carbon-FRCM systems were more effecient than PBO- and glass-FRCM counterparts in improving the structural performance of RC beams.

References

1. Younis, A.; Ebead, U. A.; Nanni, A. A Perspective on Seawater/FRP Reinforcement in Concrete Structures. In *Proceedings of the Ninth International Structural Engineering and Construction Conference, Resilient Structures and Sustainable Construction*; ISEC Press: Valencia, Spain, 2017; p. St-38.

2. Ebead, U. Inexpensive Strengthening Technique for Partially Loaded Reinforced Concrete Beams: Experimental Study. *Journal of materials in civil engineering* **2015**, *11*, 1–11, doi:10.1061/(ASCE)MT.1943-5533.0001249.

3. Baky, H. A.; Ebead, U. A.; Neale, K. W. Flexural and interfacial behavior of FRP-strengthened reinforced concrete beams. *Journal of Composites for Construction* **2007**, *11*, 629–639.

4. Ebead, U. Hybrid externally bonded/mechanically fastened fiber-reinforced polymer for RC beam strengthening. *ACI Structural Journal* **2011**, *108*, 669.

5. Ebead, U.; Marzouk, H. Fiber-reinforced polymer strengthening of two-way slabs. *ACI Structural Journal* **2004**, *101*, 650–659.

6. Elsayed, W. E.; Ebead, U. A.; Neale, K. W. Mechanically fastened FRP-strengthened two-way concrete slabs with and without cutouts. *Journal of Composites for Construction* **2009**, *13*, 198–207.

7. Kotynia, R.; Abdel Baky, H.; Neale, K. W.; Ebead, U. A. Flexural strengthening of RC beams with externally bonded CFRP systems: Test results and 3D nonlinear FE analysis. *Journal of Composites for Construction* **2008**, *12*, 190–201.

8. Ebead, U. A.; Saeed, H. Flexural and Interfacial Behavior of Externally Bonded/Mechanically Fastened Fiber-Reinforced Polymer Strengthened Reinforced Concrete Beams. *ACI Structural Journal* **2014**, *111*, 741–752.

9. Awani, O.; El-Maaddawy, T.; Ismail, N. Fabric-reinforced cementitious matrix: A promising strengthening technique for concrete structures. *Construction and Building Materials* **2017**, *132*, 94–111.

10. Shrestha, K. C.; Ebead, U.; Younis, A. Effect of Surface Roughening on Concrete/FRCM Bond. In *Proceedings of the Ninth International Structural Engineering and Construction Conference, Resilient Structures and Sustainable Construction*; ISEC Press: Valencia, Spain, 2017; p. St-43.

11. Loreto, G.; Leardini, L.; Arboleda, D.; Nanni, A. Performance of RC slab-type elements strengthened with fabric-reinforced cementitious-matrix composites. *Journal of Composites for Construction* **2013**, *18*, A4013003.

12. Ombres, L.; Verre, S. Structural behaviour of fabric reinforced cementitious matrix (FRCM) strengthened concrete columns under eccentric loading. *Composites Part B: Engineering* **2015**, *75*, 235–249.

13. Colajanni, P.; Fossetti, M.; Macaluso, G. Effects of confinement level, cross-section shape and corner radius on the cyclic behavior of CFRCM confined concrete columns. *Construction and Building Materials* **2014**, *55*, 379–389.

14. Ombres, L. Concrete confinement with a cement based high strength composite material. *Composite*

Structures **2014**, *109*, 294–304.

15. Ebead, U.; Shrestha, K. C.; Afzal, M. S.; El Refai, A.; Nanni, A. Effectiveness of fabric-reinforced cementitious matrix in strengthening reinforced concrete beams. *Journal of Composites for Construction* **2017**, *21*, 4016084.

16. Elghazy, M.; El Refai, A.; Ebead, U. A.; Nanni, A. Effect of corrosion damage on the flexural performance of RC beams strengthened with FRCM composites. *Composite Structures* **2017**, *180*, doi:10.1016/j.compstruct.2017.08.069.

17. Loreto, G.; Babaeidarabad, S.; Leardini, L.; Nanni, A. RC beams shear-strengthened with fabric-reinforced-cementitious-matrix (FRCM) composite. *International Journal of Advanced Structural Engineering (IJASE)* **2015**, *7*, 341–352.

18. Younis, A.; Ebead, U.; Shrestha, K. C. Different FRCM systems for shear-strengthening of reinforced concrete beams. *Construction and Building Materials* **2017**, *153*, 514–526, doi:10.1016/j.conbuildmat.2017.07.132.

19. Wakjira, T. G.; Ebead, U. Hybrid NSE/EB technique for shear strengthening of reinforced concrete beams using FRCM: Experimental study. *Construction and Building Materials* **2018**, *164*, 164–177, doi:10.1016/j.conbuildmat.2017.12.224.

20. Younis, A.; Ebead, U. A.; Shrestha, K. C. FRCM Shear Strengthening for Concrete Beams. In *Proceedings of the Ninth International Structural Engineering and Construction Conference, Resilient Structures and Sustainable Construction*; ISEC Press: Valencia, Spain, 2017; p. St-27.

21. ACI Committee 549 *Guide to design and construction of externally bonded fabric-reinforced cementitious matrix (FRCM) systems for repair and strengthening concrete and masonry structures (ACI 549.4R-13).*; American Concrete Institute: Farmington Hills, MI, USA., 2013; ISBN 9780870318528.

22. Younis, A.; Ebead, U. A.; Shrestha, K. C. Tensile Characterization of Textile Reinforced Mortar. In *Proceedings of the Ninth International Structural Engineering and Construction Conference, Resilient Structures and Sustainable Construction*; ISEC Press: Valencia, Spain, 2017; p. St-28.

23. Carozzi, F. G.; Poggi, C. Mechanical properties and debonding strength of Fabric Reinforced Cementitious Matrix (FRCM) systems for masonry strengthening. *Composites Part B: Engineering* **2015**, *70*, 215–230, doi:10.1016/j.compositesb.2014.10.056.

24. ISE/104 Committee *BS 4449:2005: Steel for the reinforcement of concrete. Weldable reinforcing steel. Bar, coil and decoiled product*; BSI, 2005; ISBN 978 0 580 92715 7.

25. SIKA *Technical datasheet, SikaWrap-350G Grid data sheet.*; 2016;

26. Ruredil *Technical datasheet, Ruredil X mesh C10 data sheet.*; 2016;

27. Ruredil *Technical datasheet, Ruredil X mesh gold data sheet.*; 2016;

28. International Code Council *Acceptance criteria for masonry and concrete strengthening using fabric-reinforced cementitious matrix (FRCM) composite systems (AC434).*; Washington, DC, 2013;